Running head: PD98059-induced motility in renal cancer cells.

Long-term exposure of human renal carcinoma cells to PD98059 induces epithelial-mesenchymal transition-like phenotype and enhanced motility

Shigeru Kanda[1, 3], Hiroshi Kanetake[2], and Yasuyoshi Miyata[2]

[1]Department of Molecular Microbiology and Immunology, and [2]Department of Urology, Nagasaki University Graduate School of Biomedical Science, 1-7-1, Sakamoto, Nagasaki, Japan, and [3]Department of Clinical and Experimental Laboratory Medicine, National Hospital Organization, Nagasaki Hospital, 41-6 Sakuragi, Nagasaki, Japan

Correspondence to:

Shigeru Kanda, M.D., Ph.D.,

Department of Clinical and Experimental Laboratory Medicine,

National Hospital Organization, Nagasaki Hospital

41-6 Sakuragi, Nagasaki 850-8523, Japan

Phone: +81 (95) 823-2261

Fax: +81 (95) 828-2616

E-mail: skanda-jua@umin.net

Abstract

Extracellular signal-regulated kinases (ERK) have fundamental roles in tumor progression. However, human clinical trials have shown little or no effect of inhibitors of their upstream signaling molecule, mitogen-activated protein kinase/ERK kinase (MEK), in advanced cancers. To determine the molecular mechanism underlying the limited antitumor effect, we cultured two human renal carcinoma cell lines, ACHN cells and VMRC-RCW cells in the presence of a MEK inhibitor PD98059 for more than 4 weeks (PD98059-exposed cells). PD98059-exposed ACHN cells showed elongated cell shape with scattering morphology, increase in vimentin expression, loss of β-catenin junctional localization, stress fiber formation, and increased motility. In contrast, VMRC-RCW cells showed scattered phenotype without PD98059-treatment and this treatment failed to increase the expression of vimentin. Rho A activity was increased in PD98059-exposed ACHN cells. In these cells, enhanced stress fiber formation and motility were observed, both of which were inhibited by treatment with small interfering RNA for Rho A or a Rho kinase inhibitor Y27632. Our results suggest that long-term exposure of human renal carcinoma cells to PD98059 increases cell motility by upregulating Rho A-Rho kinase signaling.

Key words: MEK inhibitor; renal carcinoma cells; Rho; stress fiber formation; motility

Introduction

Extracellular signal-regulated kinases (ERK) 1 and 2, activated by mitogen-activated protein kinase (MAPK)/ERK kinase (MEK), play essential roles in tumor progression and angiogenesis [1, 2]. In particular, activated ERK contributes to tumor cell motility [3]. MEK 1 and 2 are the only upstream molecules that can activate ERK; thus, inhibition of MEK exclusively attenuates ERK activity [4]. In human cancer cells, ERK is more highly activated than it is in normal adjunct cells [5]. However, clinical trials have shown that the use of MEK inhibitors as a treatment for advanced cancer do not adequately improve survival [6, 7]. The reason for the poor outcome of MEK inhibitor therapy in patients with cancer is not clear. The low sensitivity of malignant cells to MEK inhibitors was noted in two previous studies to be due to upregulation of K-Ras or mutation of B-Raf [8, 9]. In addition, we found that long-term exposure of human renal carcinoma cells (ACHN cells) and hormone-refractory prostate cancer cells (DU145 cells) to PD98059, a MEK inhibitor, reduced their proliferation sensitivity to PD98059 by upregulation of ERK2 protein [10]. Interestingly, we observed in that study [10] that PD98059-treated ACHN cells exhibited an elongated and fibroblastic morphology with scattered phenotype. These morphological changes are frequently observed in epithelial-mesenchymal transition (EMT), a process involved in tumor cell invasion and metastasis [11, 12].

The present study was designed to explore the molecular mechanisms underlying EMT-like changes and associated cellular responses in ACHN cells during long-term exposure to PD98059.

Materials and methods

Materials

Anti–pan-cytokeratin monoclonal antibody (C11), anti-Rho A monoclonal antibody (26C4), anti-E-cadherin (G-10), anti-β-catenin (H-102), and non-targeting control small interfering RNA (siRNA) were purchased from Santa Cruz Biotechnologies (Santa Cruz, CA). Hs_RHOA_6 and _7 HP Validated siRNA, and HiPerFect transfection reagent were obtained from QIAGEN. K. K. (Tokyo, Japan). Anti-vimentin monoclonal antibody (V9) was purchased from Chemicon International (Temecula, CA). Anti-human vinculin monoclonal antibody, TRITC-conjugated phalloidin, minimal essential medium (MEM), and non-essential amino acids (NEAA) were purchased from Sigma Chemical Company (St. Louis, MO). Rhotekin Rho binding domain (RBD)-glutathione S-transferase (GST) fusion protein coupled to agarose beads was obtained from Upstate Cell Signaling Solutions (Temecula, CA). Fetal bovine serum (FBS) was obtained from Invitrogen Corporation (Carlsbad, CA). Y27632 was obtained from Merck Bioscience (Calbiochem, La Jolla, CA). PD98059 (Wako Pure Chemicals, Osaka, Japan) was dissolved in dimethyl sulfoxide (DMSO) and stored at -80°C until use. After thawing, it was dissolved in the culture medium and added to the cells. The final concentration of DMSO was 0.1%.

Cell culture

Human renal carcinoma cell lines, ACHN cells and VMRC-RCW cells [13], were cultured in MEM supplemented with NEAA and 10% FBS. For long-term exposure of cells to PD98059, the cells were continuously cultured in the presence of 50 μM PD98059 for more than 4 weeks.

Unexposed parental cells were designated as $ACHN_{pa}$ and $VMRC\text{-}RCW_{pa}$ cells, respectively, and cells chronically exposed to PD98059 were designated as $ACHN_{PD}$ cells and $VMRC\text{-}RCW_{PD}$ cells, respectively.

Immunoblotting

Cells were grown in 24-well plates. Two sets of cultures were prepared: one set was used for immunoblotting and the other set was used for cell counts. The culture medium for cells chronically treated with PD98059 was always supplemented with 50 μM PD98059. Cells were lysed by boiled SDS-sample buffer, and the proteins from equal number of cells in each lysate were separated on SDS polyacrylamide gels. Proteins were electrotransferred onto polyvinylidene difluoride (PVDF) membranes (Millipore, Bedford, MA). Membranes were incubated with the indicated antibodies, followed by incubation with peroxidase-conjugated secondary antibodies. Proteins were visualized using enhanced chemiluminescence reagents (Pierce Biotechnology, Rockford, IL) and exposed on X-ray films. The membranes were stripped between two probings, as described previously [14].

Indirect immunofluorescent staining

Indirect immunofluorescent staining was performed as described previously [15]. Cells were seeded onto the surface of coverslips with or without PD98059 and cultured for2 days. Cells were washed with PBS, fixed with 3.7% paraformaldehyde, and permeabilized with 0.05% Triton X-100. After the blocking of nonspecific protein binding with PBS supplemented with 5% dry milk and 10% goat serum, cells were stained with anti-E-cadherin monoclonal antibody or anti-β-catenin polyclonal antibody. Primary antibodies were visualized with

corresponding secondary antibodies labeled with biotin, followed by the incubation with streptoavidin-Alexa Fluor 555 conjugates.

Examination of stress fiber formation

Stress fiber formation was determined as described previously [13]. In brief, cells (2×10^4 cells/well) were seeded onto cover slips in 24-well plates and cultured for 20 h. They were then incubated in a serum-free medium for 3 h and either stimulated with 10% FBS for 20 min or left unstimulated. Cells were then fixed with 3.7% paraformaldehyde in phosphate-buffered saline (PBS) for 20 min at room temperature, followed by incubation with 0.1% Triton X-100 in Tris-buffered saline (TBS) for 3 min. Cells were washed with TBS and incubated with TRITC-conjugated phalloidin for 20 min. After washing and mounting, photographs were taken under a fluorescence microscope.

Chemokinesis assay

To quantify cell migration, we performed the chemokinesis assays [13]. Briefly, cells were suspended in a serum-free medium and placed onto the upper surface of the membranes of Transwell inserts (6.7-mm in diameter, 8-μm pore) pre-coated with bovine type I collagen (30 mg/ml) at a density of 1.5×10^4 cells/membrane. The inserts were then placed in wells containing serum-free medium with or without 10% FBS. The culture medium of cells treated with PD98059 for more than 4 weeks was always supplemented with 50 μM PD98059. The cells were incubated for 24 h and fixed with 100% methanol. Cells on the upper surface were removed by cotton swabs, while those that migrated to the surface of the lower membrane of the Transwell inserts were stained with Giemza solution and counted microscopically.

Assay for Rho A activity

The GTP-bound active form Rho A was precipitated from the indicated cell lysate with Rhotekin RBD-GST conjugated beads using the protocol provided by the manufacturer. $ACHN_{pa}$ cells or $ACHN_{PD}$ cells were cultured in the presence of 10% FBS and lysed in the Mg^{2+} lysis buffer [25 mM N-2-hydroxyetylpiperazine-N'-ethanesulphonic acid (HEPES), pH 7.5, 150 mM NaCl, 1% Igepal CA-630, 10 mM $MgCl_2$, 1 mM ethylenediaminetetraacetic acid (EDTA), and 2% glycerol]. Ninety percent of lysate was incubated with Rhotekin RBD-GST conjugated beads and bound proteins were separated on SDS-polyacrylamide gels, followed by transfer onto polyvinylidene fluoride (PVDF) membranes (Millipore, Bedford, MA). Rho A protein was detected by immunoblotting as described above. The remaining 10% lysate was examined for the loaded amount of proteins.

Treatment of cells with siRNA

Treatment of cells with siRNA (25 nM each) was described previously [10]. Briefly, $ACHN_{PD}$ cells were cultured in wells of 24-well plates. The culture medium was replaced with a fresh medium containing 10% FBS. A serum-free medium supplemented with HiPerFect reagent and control siRNA, or either Hs_RHOA_6 or _7 HP Validated siRNA at 25 nM, was added to the cells. After 2 days, the cells were detached and their number counted. A portion of the suspended cells was used for chemokinesis assay and the remaining cells were examined for the expression of Rho A proteins by immunoblotting as described above.

Statistical analysis

Values are presented as mean cell numbers ± SD. Differences between two groups were analyzed using the Mann-Whitney U test. Differences were considered significant when $P < 0.05$.

Results

Long-term exposure to PD98059 induces EMT-like phenotype of ACHN cells

ACHN cells grow as a compact seat with cell-cell contact, whereas VMRC-RCW cells grow without cell-cell contact (scattered morphology) [13]. We first examined the effect of short-term PD98059 treatment on serum-activated ERK in these cells. As shown in Fig. 1, serum-treatment activated ERK in these cells with similar kinetics and treatment with PD98059 strongly inhibited the activation. This result suggests that PD98059 used in this study is active against ERK activation. We then cultured these cells in the presence or absence of 50 μM of PD98059 for more than 4 weeks. As shown in Fig. 2A, $ACHN_{PD}$ cells showed an elongated cell shape with scattered morphology, whereas long-term exposure to PD98059 did not induce any morphological changes in $VMRC\text{-}RCW_{PD}$ cells (Fig. 2C). Next, we prepared total cell extracts and determined the expression of cytokeratin (a marker of epithelial cells) and vimentin (a marker of mesenchymal cells). As shown in Fig. 2B, expression of cytokeratin was not altered in $ACHN_{PD}$ cells. In contrast, expression of vimentin was increased in these cells. In VMRC-RCW cells, no such alteration was observed (Fig. 2D). Long-term treatment of ACHN cells with PD98059 reduced their growth sensitivity to PD98059 treatment through upregulation of ERK 2 (10). Upregulation of ERK was observed in both $ACHN_{PD}$ cells and $VMRC\text{-}RCW_{PD}$ cells (Fig. 2D) and the decrease in growth sensitivity to PD98059 was also observed in these cells (data not shown). We also examined the expression of E-cadherin and β-catenin in these cells assessed by immunoblotting. However, no alteration of the expression of these proteins was observed (data not shown). Because the expression of E-cadherin in these cells was relatively low, we investigated the localization of β-catenin in ACHN cells. As shown in Fig. 2 E, β-catenin was localized at the site of cell-cell contact

(junctional localization). Chronic exposure to PD98059 disrupted the junctional localization of β-catenin. These results suggest that long-term exposure of ACHN cells to PD98059 induces EMT-like phenotype. This phenotype was reversible because culture of $ACHN_{PD}$ cells in the absence of PD98059 for 2 weeks reverted the morphological changes as well as expression of vimentin (data not shown).

The EMT-like phenotype of $ACHN_{PD}$ cells is associated with enhanced cell motility

EMT is involved in metastatic progression of tumor cells partly by enhanced cell motility [11, 12]. We examined stress fiber formation in $ACHN_{pa}$ and (PD) cells. As shown in Fig. 3A, FBS-treatment induced stress fiber formation in $ACHN_{pa}$ cells. In contrast, $ACHN_{PD}$ cells showed enhanced stress fiber formation in the absence of FBS. FBS-treatment induced lamellipodia formation in these cells. We also examined the random motility of these cells by the chemokinesis assay. As shown in Fig. 3B, chemokinesis of $ACHN_{pa}$ cells was stimulated by treatment with FBS. Chemokinesis of $ACHN_{PD}$ cells was significantly higher than that of $ACHN_{pa}$ cells in the absence of FBS and FBS did not further stimulate cell migration. These results suggest that the EMT-like phenotype of $ACHN_{PD}$ cells is associated with enhanced cell motility, which may increase their metastatic potential *in vivo*.

Elevated Rho A activity may be responsible for PD98059-induced EMT in ACHN cells

Previous studies showed that inhibition of ERK pathway in cancer cells resulted in upregulation of Rho-Rho kinase signaling [16, 17]. There is also evidence for the involvement of Rho signaling in EMT [11, 12]. Rho A regulates stress fiber formation, whereas Rac and Cdc42 regulate lamellipodia and filopodia, respectively [18, 19]. We first examined the

activity of Rho A in ACHN$_{pa}$ and ACHN$_{PD}$ cells. As shown in Fig. 4A, increased binding of active Rho A to RBD-GST fusion protein was observed in ACHN$_{PD}$ cells compared with parental cells. Rac and Cdc42 activities were not upregulated in ACHN$_{PD}$ cells (data not shown). The difference of Rho A activity between VMRC-RCW$_{pa}$ cells and VMRC-RCW$_{PD}$ cells was not observed (data not shown). FBS-treatment increased activated Rho A in ACHN$_{pa}$ cells, but not in ACHN$_{PD}$ cells (data not shown). These observations were compatible with the enhanced stress formation without lamellipodia and filopodia observed in ACHN$_{PD}$ cells. We next examined the effect of downregulation of endogenous Rho A by siRNA on ACHN$_{PD}$ cells. As shown in Fig. 4B, Hs_RHOA_6 HP Validated siRNA efficiently downregulated the expression of Rho A in ACHN$_{PD}$ cells. Treatment of the cells with the same siRNA inhibited stress fiber formation and chemokinesis (Fig. 4C and D). Treatment of the cells with Hs_RHOA_7 HP Validated siRNA showed similar results (data not shown). We also examined the effect of Y27632, a Rho kinase inhibitor, on morphological change in ACHN$_{PD}$ cells. As shown in Fig. 5A, Y27632 reverted the elongated morphology. Treatment of these cells with Y27632 also inhibited stress fiber formation and chemokinesis (Fig. 5B and C). These results suggest that elevated Rho A-Rho kinase signaling may be responsible for the EMT-like phenotype and increased motility of ACHN$_{PD}$ cells.

Discussion

Since ERK is involved in a variety of tumor cell responses, inhibition of ERK was expected as a potential strategy in the treatment of advanced cancer. Inhibition of MEK 1 and 2, upstream signaling molecules of ERK, specifically and efficiently inhibits ERK activity. Thus, a number of small molecular weight synthetic inhibitors have been tested their activities against tumor cell responses in vitro and tumor progression in vivo. Among them, CI-1040, was found to inhibit ERK activity both in vitro and in vivo, and was well tolerated, although it provided little benefits for patients with advanced cancers [6, 7]. Therefore, resistance of tumor cells to long-term ERK inhibition allowed tumor cells to proliferate and survive during such therapy. It is also plausible that long-term ERK inhibition may induce aggressive phenotypes of tumor cells. In the present study, we showed for the first time that long-term exposure of human renal carcinoma cells to PD98059 induced an increase in stress fiber formation and cell motility. These responses were associated with elongated and scattered morphology, upregulation of vimentin, and a loss of β-catenin junctional localization; changes that are observed in EMT [11]. We failed to observe the downregulation of the expression of E-cadherin and β-catenin by chronic treatment with PD98059 in ACHN cells. Similar results were reported with transforming growth factor-β (TGF-β)-induced EMT in NMuMG breast epithelial cells [20]. However, a loss of E-cadherin junctional localization was demonstrated in response to TGF-β-treatment [20]. Similarly, a loss of β-catenin junctional localization was observed in the present study (Fig. 2 E). We also observed the similar phenotypes including morphology, stress fiber formation, and enhanced motility in ACHN cells chronically treated with U0126 (unpublished observation). Thus, long-term inhibition of ERK in human cancer may stimulate local invasion and metastasis of certain tumor cells.

In the present study, stress fiber formation and motility of another human renal carcinoma cells, VMRC-RCW cells, were not stimulated by the long-term treatment with PD98059. This treatment, however, upregulated the expression of ERK and reduced the sensitivity of proliferative activity to PD98059, which were observed in $ACHN_{PD}$ cells (Fig. 2D and data not shown). Therefore, it seems likely that upregulation of ERK is a fundamental response, whereas enhanced stress fiber formation and cell motility may be a cell type-specific response in tumor cells chronically treated with PD98059. The mechanism underlying the lack of enhanced stress fiber formation and motility in VMRC-RCW cells is not clear at present. One possibility is that Rho A activity in these cells might be already increased before long-term exposure to PD98059. Nakamura et al. [13] reported that VMRC-RCW cells showed increased PI3-kinase activity by overexpression of hepatocyte growth factor receptor and subsequent ligand-independent activation of its tyrosine kinase activity. Motility of VMRC-RCW cells was inhibited by LY294002 [13]. Thus, the status of PI3-kinase activity may reflect stress fiber formation and motility of tumor cells following long-term treatment with PD98059.

The motility of tumor cells is positively regulated by several other signaling molecules, such as Src family kinases, phosphoinositide 3-kinase (PI3-kinase), and ERK [3, 21, 22]. However, Src inhibitor, PP2, or PI3-kinase inhibitor, LY294002, failed to inhibit stress fiber formation and chemokinesis by $ACHN_{PD}$ cells (data not shown). We reported previously that overexpression of ERK 2 was associated with reduced proliferation sensitivity to PD98059 in $ACHN_{PD}$ cells [10]. However, downregulation of ERK 2 by specific siRNA also failed to inhibit stress fiber formation and chemokinesis by these cells (data not shown). In $ACHN_{PD}$ cells, Rho A activity was increased compared to its parental cells (Fig. 4A). The increased stress fiber formation and motility of these cells were dependent on Rho A-Rho kinase activity, because these cellular responses were inhibited by treatment with Rho A siRNA to downregulate the expression of Rho A or Rho kinase inhibitor Y27632 (Figs. 4 and 5).

Extrapolation of these results to a clinical setting suggests that the combination of MEK inhibitors and Rho kinase inhibitors may enhance the antitumor activity of the former and be potentially useful in the treatment of patients with advanced cancers.

Acknowledgments

We are grateful to T. Shimogama for the skilled help. This work was supported by a Grant-in-Aid from the Japan Society for the Promotion of Science.

References

1. Pouysségur J, Lenormand P (2003) Fidelity and spatio-temporal control in MAP kinase (ERKs) signalling. Eur J Biochem 270:3291-3299
2. Reddy KB, Nabha SM, Atanaskova N (2003) Role of MAP kinase in tumor progression and invasion. Cancer Metastasis Rev 22:395-403
3. Huang C, Jacobson K, Schaller MD (2004) MAP kinases and cell migration. J Cell Sci 117:4619-4628
4. Kohno M, Pouysségur J (2003) Pharmacological inhibitors of the ERK signaling pathway: application as anticancer drugs. Prog Cell Cycle Res 5:219-224
5. Hoshino R, Chatani Y, Yamori T, Tsuruo T, Oka H, Yoshida O, Shimada Y, Ari-i S, Wada H, Fujimoto J, Kohno M (1999) Constitutive activation of the 41-/43-kDa mitogen-activated protein kinase signaling pathway in human tumors. Oncogene 18:813-822
6. Rinehart J, Adjei AA, Lorusso PM, Waterhouse D, Hecht JR, Natale RB, Hamid O, Varterasian M, Asbury P, Kaldjian EP, Gulyas S, Mitchell DY, Herrera R, Sebolt-Leopold JS, Meyer MB (2004) Multicenter phase II study of the oral MEK inhibitor, CI-1040, in patients with advanced non-small-cell lung, breast, colon, and pancreatic cancer. J Clin Oncol 22:4456-4462
7. Lorusso PM, Adjei AA, Varterasian M, Gadgeel S, Reid J, Mitchell DY, Hanson L, DeLuca P, Bruzek L, Piens J, Asbury P, Van Becelaere K, Herrera R, Sebolt-Leopold J, Meyer MB (2005) Phase I and pharmacodynamic study of the oral MEK inhibitor CI-1040 in patients with advanced malignancies. J Clin Oncol 23:5281-5293

8. Wang Y, Van Becelaere K, Jiang P, Przybranowski S, Orner C, Sebolt-Leopold J (2005) A role for K-ras in conferring resistance to the MEK inhibitor, CI-1040. Neoplasia 7:336-347
9. Solit DB, Garraway LA, Pratilas CA, Sawai A, Getz G, Basso A, Ye Q, Lobo JM, She Y, Osman I, Golub TR, Sebolt-Leopold J, Sellers WR, Rosen N (2006) BRAF mutation predicts sensitivity to MEK inhibition. Nature 439:358-362
10. Kanda S, Kanetake H, Miyata Y (2006) Elevated expression of ERK 2 in human tumor cells chronically treated with PD98059. Biochem Biophys Res Commun 345: 1481-1486
11. Lee JM, Dedhar S, Kalluri R, Thompson EW (2006) The epithelial-mesenchymal transition: new insights in signaling, development, and disease. J Cell Biol 172: 973-981
12. Thiery JP, Sleeman JP (2006) Complex networks orchestrate epithelial-mesenchymal transitions. Nat Rev Mol Cell Biol 7: 131-142
13. Nakamura T, Kanda S, Kohno T, Yamamoto K, Maeda K, Matsuyama T, Kanetake H (2001) Increase in hepatocyte growth factor receptor tyrosine kinase activity in renal carcinoma cells is associated with increased motility through partly phosphoinositide 3-kinase. Oncogene 20: 7610-7623
14. Kanda S, Lerner EC, Tsuda S, Shono T, Kanetake H, Smithgall TE (2000) The nonreceptor protein-tyrosine kinase c-Fes is involved in fibroblast growth factor-2-induced chemotaxis of murine brain capillary endothelial cells. J Biol Chem 275:10105-10111
15. Kanda S, Miyata Y, Kanetake H, Smithgall TE (2006) Fibroblast growth factor-2 induces the activation of Src through Fes, which regulates focal adhesion disassembly. Exp Cell Res 312:3015-3022
16. Vial E, Sahai E, Marshall CJ (2003) ERK-MAPK signaling coordinately regulates activity of Rac1 and RhoA for tumor cell motility. Cancer Cell 4: 67-79

17. Mavria G, Vercoulen Y, Yeo M, Paterson H, Karasarides M, Marais R, Bird D, Marshall CJ (2006) ERK-MAPK signaling opposes Rho-kinase to promote endothelial cell survival and sprouting during angiogenesis. Cancer Cell 2006;9:33-44.
18. Hall A (1998) Rho GTPases and the actin cytoskeleton. Science 279: 509-514.
19. Etienne-Manneville S, Hall A (2002) Rho GTPases in cell biology. Nature 420: 629-635.
20. Bhowmick NA, Ghiassi M, Bakin A, Aakre M, Lundquist CA, Engel ME, Arteaga CL, Moses HL (2001) Transforming growth factor-beta1 mediates epithelial to mesenchymal transdifferentiation through a RhoA-dependent mechanism. Mol Biol Cell 12:27-36
21. Yin HL, Janmey PA (2003) Phosphoinositide regulation of the actin cytoskeleton. Ann Rev Physiol 65:761-789
22. Parsons SJ, Parsons JT (2004) Src family kinases, key regulators of signal transduction. Oncogene 23:7906-7909

Figure legends

Figure 1. PD98059 at 50 μM efficiently inhibits serum-induced activation of ERK in human renal carcinoma cells. Two human renal carcinoma cell lines, ACHN cells and VMRC-RCW cells, were seeded onto wells of 24-well plates and cultured for 24 h. Cells were then serum-starved overnight and a fresh serum-free medium was added with or without 50 μM PD98059 and incubated for 2 h. The indicated cells were stimulated with 10% (Vo/Vo) FBS for the indicated periods and lysed. Proteins were separated onto SDS-PAGE, followed by transfer onto PVDF membranes. Activated ERK was detected with anti-phospho-MAPK antibody. Reproducible results were obtained from two independent experiments.

Figure 2. (A) Long-term treatment of ACHN cells with 50 μM PD98059 induces EMT-like phenotype. ACHN cells were cultured for more than 4 weeks in the presence or absence of 50 μM PD98059, denoted $ACHN_{PD}$ cells and $ACHN_{pa}$ cells, respectively. Pictures were taken by a phase-contrast microscope. **(B)** Long-term exposure to 50 μM PD98059 upregulates the expression of vimentin and ERK 2 in $ACHN_{PD}$ cells. Cells were cultured in the wells of 24-well plates and proteins were extracted from their lysates. Expression of particular proteins was determined by immunoblotting with the indicated antibodies. Reproducible results were obtained from two independent experiments. **(C)** Long-term exposure of VMRC-RCW cells to 50 μM PD98059 does not induce morphological changes. VMRC-RCW cells were cultured for more than 4 weeks in the presence or absence of 50 μM PD98059, denoted $VMRC\text{-}RCW_{PD}$ cells and $VMRC\text{-}RCW_{pa}$ cells, respectively. Pictures were taken by a phase-contrast microscope. **(D)** Long-term treatment of $VMRC\text{-}RCW_{PD}$ cells with 50 μM PD98059 upregulates the expression of ERK2, but not vimentin. Cells were cultured in the well of 24-well plates and proteins were extracted from their lysates. Expression of particular proteins

was determined by immunoblotting with the indicated antibodies. Reproducible results were obtained from two independent experiments. **(E)** Long-term exposure to 50 μM PD98059 induces a loss of β-catenin junctional localization in ACHN cells. $ACHN_{pa}$ cells and $ACHN_{PD}$ cells were seeded onto coverslips and localization of β-catenin was examined by indirect immunofluorescent staining.

Figure 3. (A) Stress fiber formation in $ACHN_{pa}$ cells and $ACHN_{PD}$ cells. Cells grown on coverslips were serum-starved and left unstimulated or stimulated with 10% FBS. Cells were fixed and polymerized actin was visualized by incubation with TRITC-conjugated phalloidin. Reproducible results were obtained from three independent experiments. (**B**) Chemokinesis of $ACHN_{pa}$ cells and $ACHN_{PD}$ cells. Cells were suspended in MEM and NEAA with or without 10% FBS and were seeded onto the upper surface of Transwell inserts pre-coated with type I collagen. The inserts were then placed in wells containing MEM and NEAA with or without 10% FBS. Either 0.1% DMSO ($ACHN_{pa}$ cells) or 50 μM PD98059 ($ACHN_{PD}$ cells) was added to the culture medium in both the upper and lower wells. After 24 h, the cells were fixed, and those that had migrated to the lower membrane surface of Transwell inserts were stained with Giemza solution and counted microscopically. Data are the mean number of cells ± SD of four wells. Reproducible results were obtained from two independent experiments.

Figure 4. (A) Rho A activity is higher in $ACHN_{PD}$ cells than in $ACHN_{pa}$ cells. The active form Rho A was precipitated from 90% of either $ACHN_{pa}$ or $ACHN_{PD}$ cell lysate with Rhotekin RBD-GST conjugated beads, separated onto SDS-PAGE and precipitated Rho A was detected by immunoblotting. The remaining 10% lysate was used for the examination of loaded protein by immunoblotting with anti-Rho A and anti-vinculin antibodies. Reproducible results were obtained from two independent experiments. **(B)** Expression of Rho A in $ACHN_{PD}$ cells is

downregulated by treatment with Rho A siRNA. Cells grown in 24-well plates were treated with the indicated siRNA. Two days later, the cells were lysed and proteins from 1×10^4 cells were examined for Rho A expression by immunoblotting. Immunoblotting with anti-vinculin antibody was performed to assess the loaded proteins. **(C)** Effect of Rho A siRNA on stress fiber formation of $ACHN_{PD}$ cells. Cells grown on coverslips were treated with the indicated siRNA. Two days later, stress fiber formation was examined as described in the legend of Fig. 3 A. Reproducible results were obtained from two independent experiments. **(D)** Effect of Rho A siRNA on chemokinesis of $ACHN_{PD}$ cells. Cells grown in 6-well plates were treated with the indicated siRNA. Two days later, the chemokinesis assay was carried out as described in the legend of Fig. 3 B. Data are mean ± SD of four wells. Reproducible results were obtained in two independent experiments.

Figure 5. (A) Effect of Y27632 on the morphology of $ACHN_{PD}$ cells. Cells grown in the well of 24-well plates were serum-starved and treated with either water (vehicle) or 10 μM Y27632 for 2 h. Pictures were taken as described in the legend of Fig. 2 A. **(B)** Effect of Y27632 on stress fiber formation of $ACHN_{PD}$ cells. Cells grown on coverslips were serum-starved and treated with either water or 10 μM Y27632 for 2 h. Stress fiber formation was examined as described in the legend for Fig. 3 A. Reproducible results were obtained from two independent experiments. (**C**) Effect of Y27632 on chemokinesis of $ACHN_{PD}$ cells. Cells suspended in serum-free medium supplemented with either water or 10 μM Y27632 were seeded onto the upper surface of Transwell inserts, and the chemokinesis assay was performed as described in the legend of Fig. 3 B. Bars represent mean cell number ± SD of four wells. Reproducible results were obtained from two independent experiments.

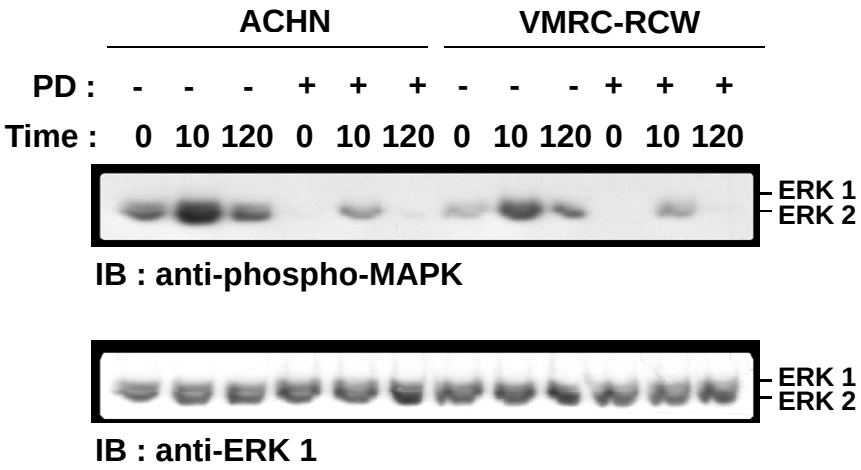

Fig. 1. by S. Kanda et al.

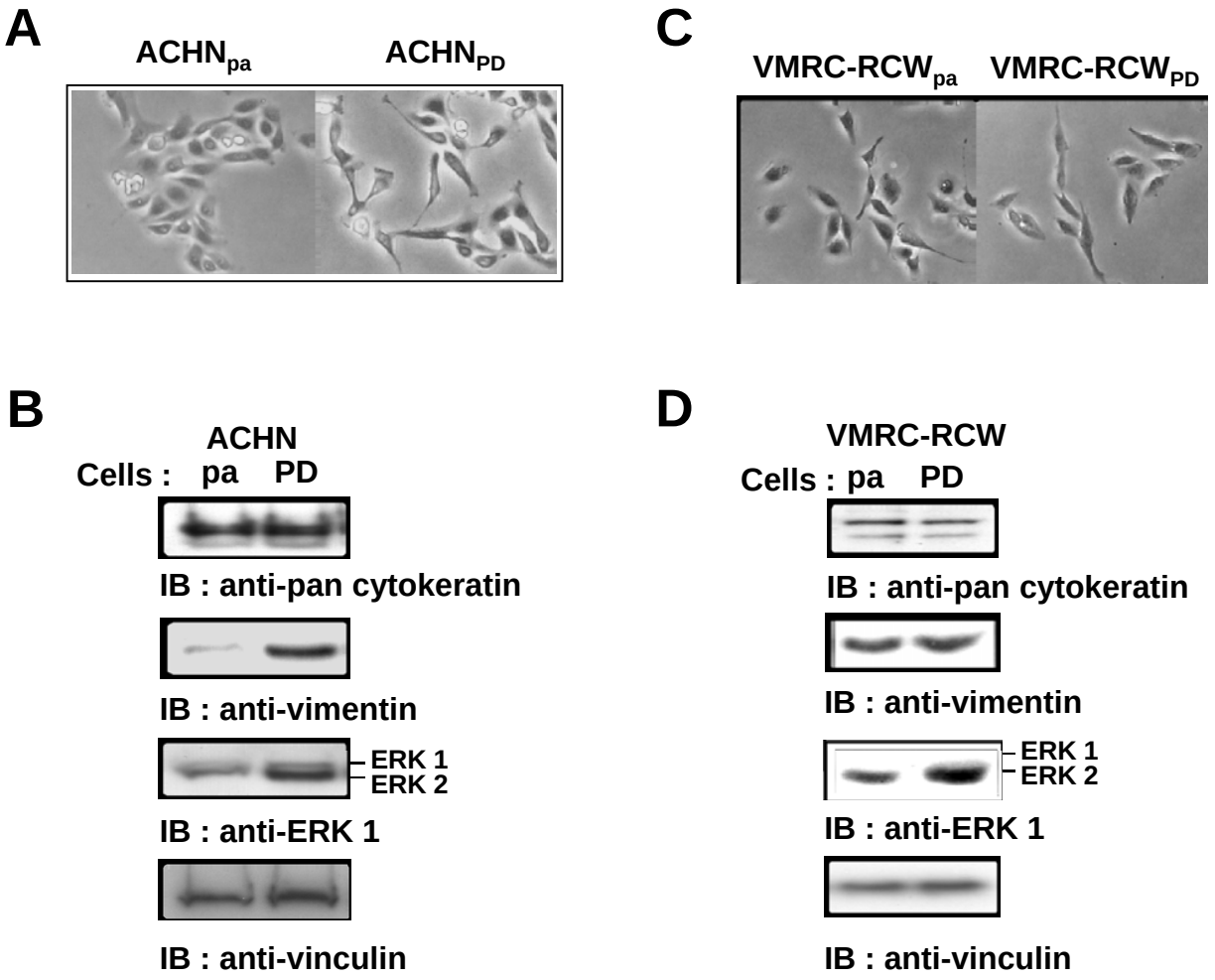

Fig. 2. by S. Kanda et al.

E

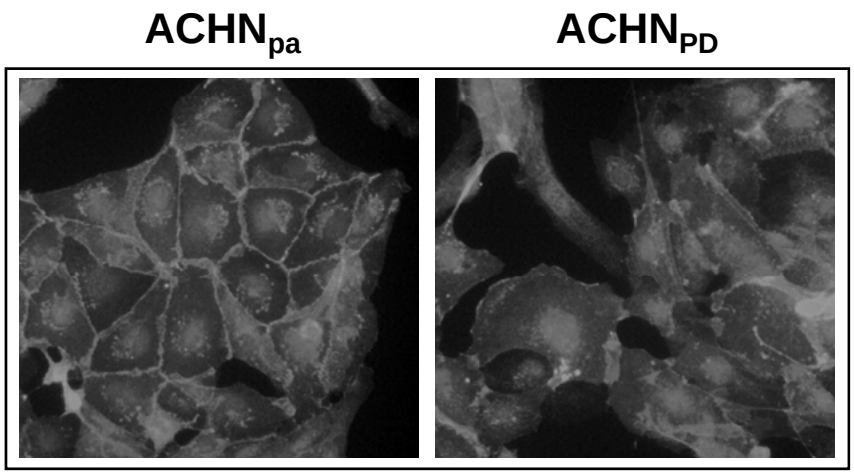

Fig. 2. by S. Kanda et al.

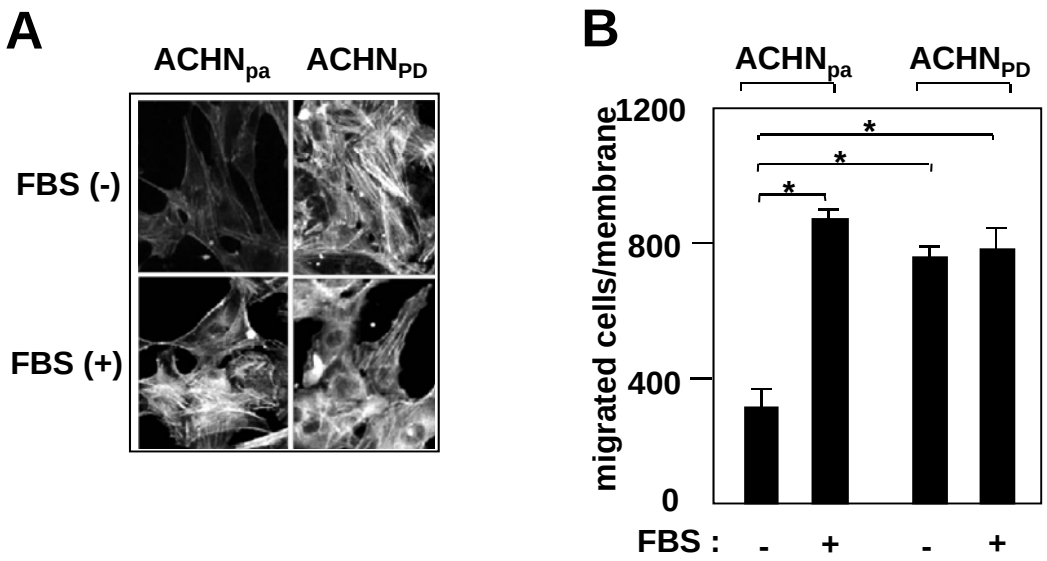

Fig. 3. by S. Kanda et al.

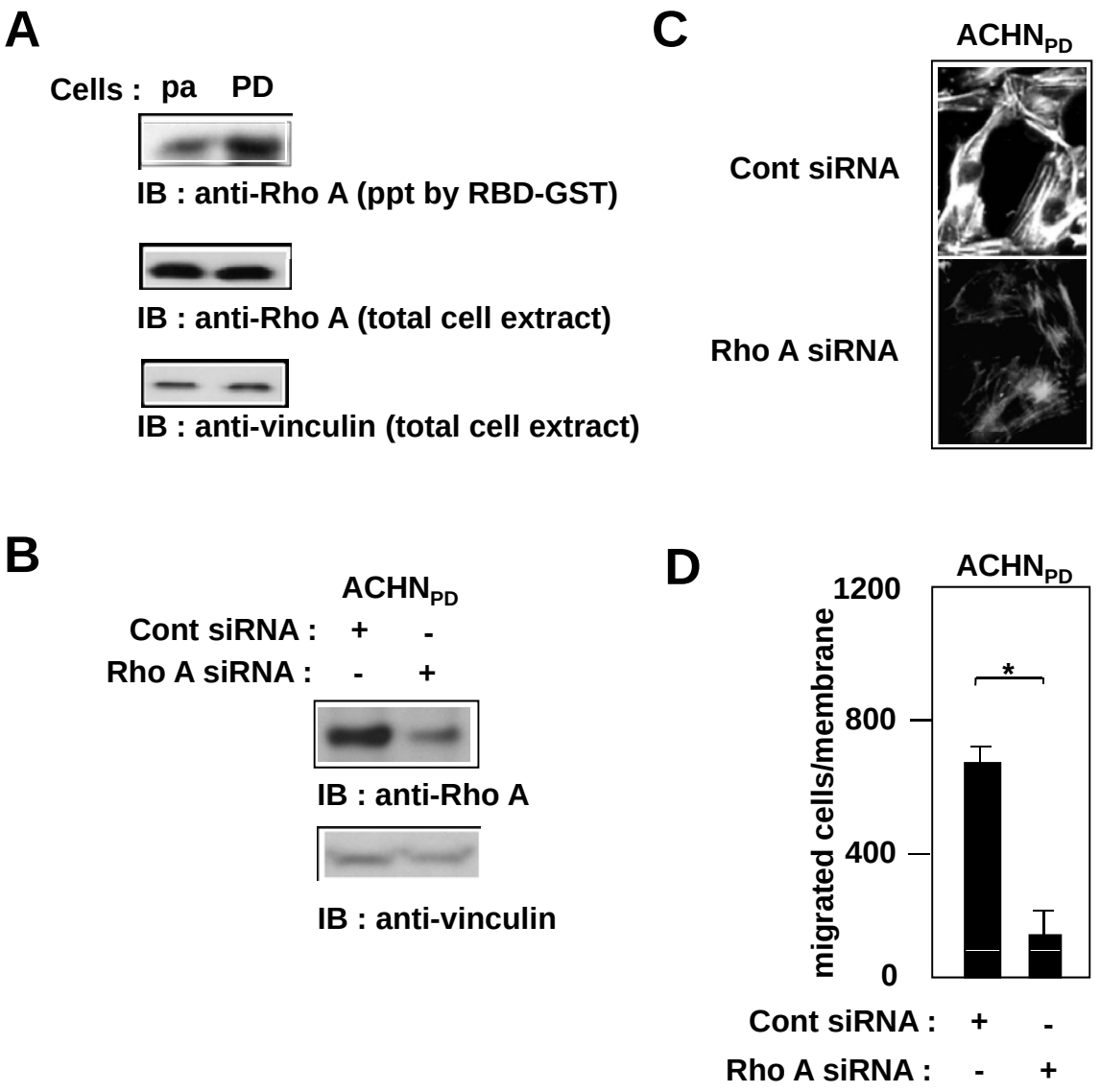

Fig. 4. by S. Kanda et al.

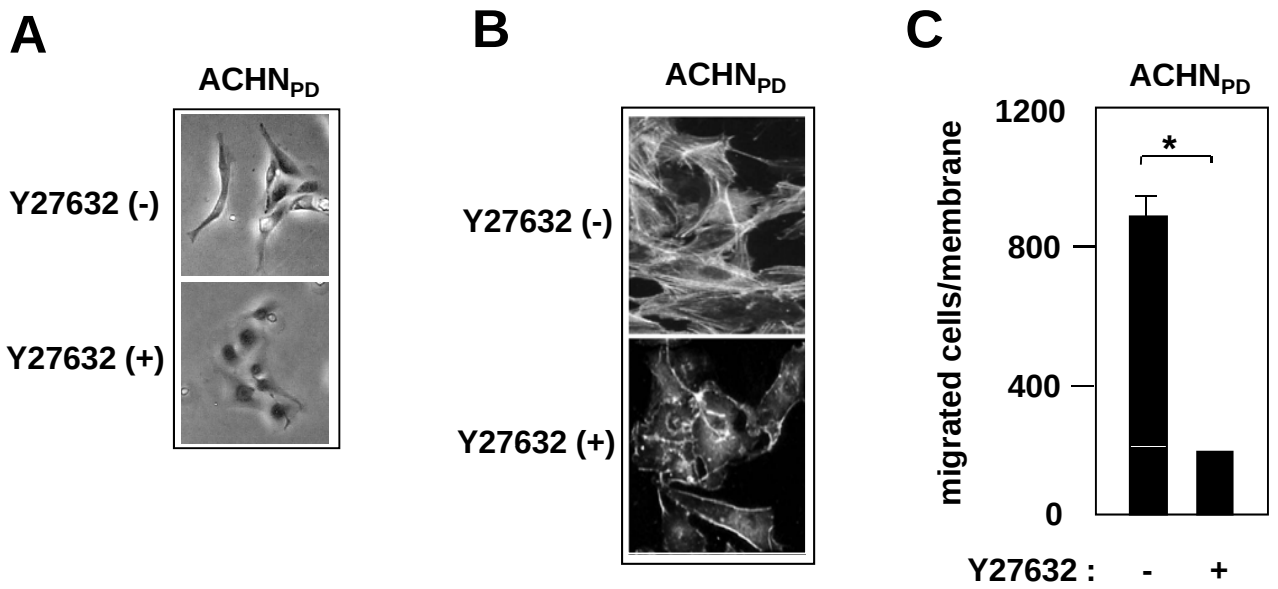

Fig. 5. by S. Kanda et al.